International Journal of Wireless Information Networks, Vol. 10, No. 4, October 2003 (© 2004)

A Generalized Signal Flow Graph Approach for Hybrid Acquisition of Ultra-Wideband Signals

Eric A. Homier[1,2] and Robert A. Scholtz

This paper establishes a general framework for the study of various search procedures in which a group of observers is searching for a group of items in some arbitrary manner. A generalized signal flow graph approach yields a complete statistical description of the search time as well as the probability of correctly terminating the search. The motivation for this study comes from the acquisition of an ultra-wideband (UWB) signal in a dense multipath channel. In this particular problem many resolvable paths tend to cluster at a receiver containing multiple correlators allowing for a hybrid serial/parallel search. This hybrid search, as well as a bound on a sorted hybrid search, is analyzed using the generalized signal flow graph approach. Rapid code and frame acquisition at the receiver is desired and it is shown that a specific nonconsecutive search, the *bit reversal search*, yields an optimum hybrid search procedure under certain conditions. The acquisition of UWB signals also leads to the concept of a self-similar signal flow graph, in which a new search is initiated upon the completion of the previous one.

KEY WORDS: Code acquisition; nonconsecutive search; ultra-wideband; synchronization.

1. INTRODUCTION

The general problem of searching for an object in some uncertainty region arises in a large number of situations. A specific example includes the acquisition process for a wireless communication system. Traditionally, however, a single observer is searching for a single object. This restriction is removed in this paper, and the general case of multiple observers searching for multiple objects is examined. For this general problem the search pattern, that is, the pattern in which the locations in the uncertainty region are examined, is of interest. Typically, a pattern is desired so as to optimize some parameter, for example, to minimize the search time or to maximize the probability of correctly ending the search. This pattern, or sequence, design problem is discussed briefly in Section 2, in which the search problem is analyzed using a generalized signal flow graph. It will be assumed throughout this paper that the uncertainty region is comprised of a finite set of bins, some subset of which contain objects that when found will terminate the search. This scenario is seen during spread spectrum, for example, CDMA or ultra-wideband (UWB), code acquisition in dense multipath channels. Initial studies in CDMA code acquisition usually neglected multipath [1], whereas recent investigation has included multipath ([2–5] and the references contained therein).

Dense multipath channels, as found in the indoor or urban environments, are characterized by many paths arriving at a single point clustered very closely in time. For narrowband systems, this generally leads to destructive interference, or spatial nulls. One advantage of UWB signals, those with large fractional bandwidths, is that the paths arriving at any one point in space are generally resolvable because of the short time duration of the transmitted signal. The UWB signal and the dense

[1] Northrop Grumman Space Technology in Redondo Beach, California, University of Southern California.
[2] E-mail: eric.homier@ngc.com.

1068-9605/03/0010-0179/0 © 2004 Plenum Publishing Corporation

multipath channel model are both discussed in Section 3. The acquisition of this time-hopped UWB signal in the multipath channel is investigated in Section 4. This includes acquisition of both the time-hopping code and the frame boundaries.

The codes considered in this paper are assumed to be short codes, that is, a single dwell time over a code period is possible in a reasonable amount of time. The use of long codes in spread spectrum systems requires the use of partial code correlations, but the search problem is still the same. In either case, a fully parallel search of the uncertainty region is often prohibitive. Thus fixed dwell time serial searches are often used as a less complex alternative to fully parallel searches. Other search techniques exist, including nonserial or variable dwell time techniques, which tend to offer slightly better performance compared to fixed dwell time serial search techniques. The cost of increased performance, however, is increased complexity in the receiver architecture [5,6]. Another method of code acquisition, which will not be discussed here, involves message passing algorithms [7]. The approach chosen here is a hybrid scheme in which some subset of bins are searched simultaneously. This is accomplished using multiple correlators, for example, the taps of a RAKE receiver. Section 5 discusses the hybrid search, and Section 6 discusses a sorted hybrid search in which the most likely bins are examined first. Section 7 briefly discusses a bound on the single observer mean search time. Finally, Section 8 discusses the process of fine acquisition.

2. GENERALIZED SEARCH ANALYSIS

The generalized signal flow graph considered in this paper is shown in Figure 1. This signal flow graph, which is an extension of the basic signal flow graph of [1], will be used to analyze the UWB acquisition. As can be seen from Figure 1, the generalized signal flow

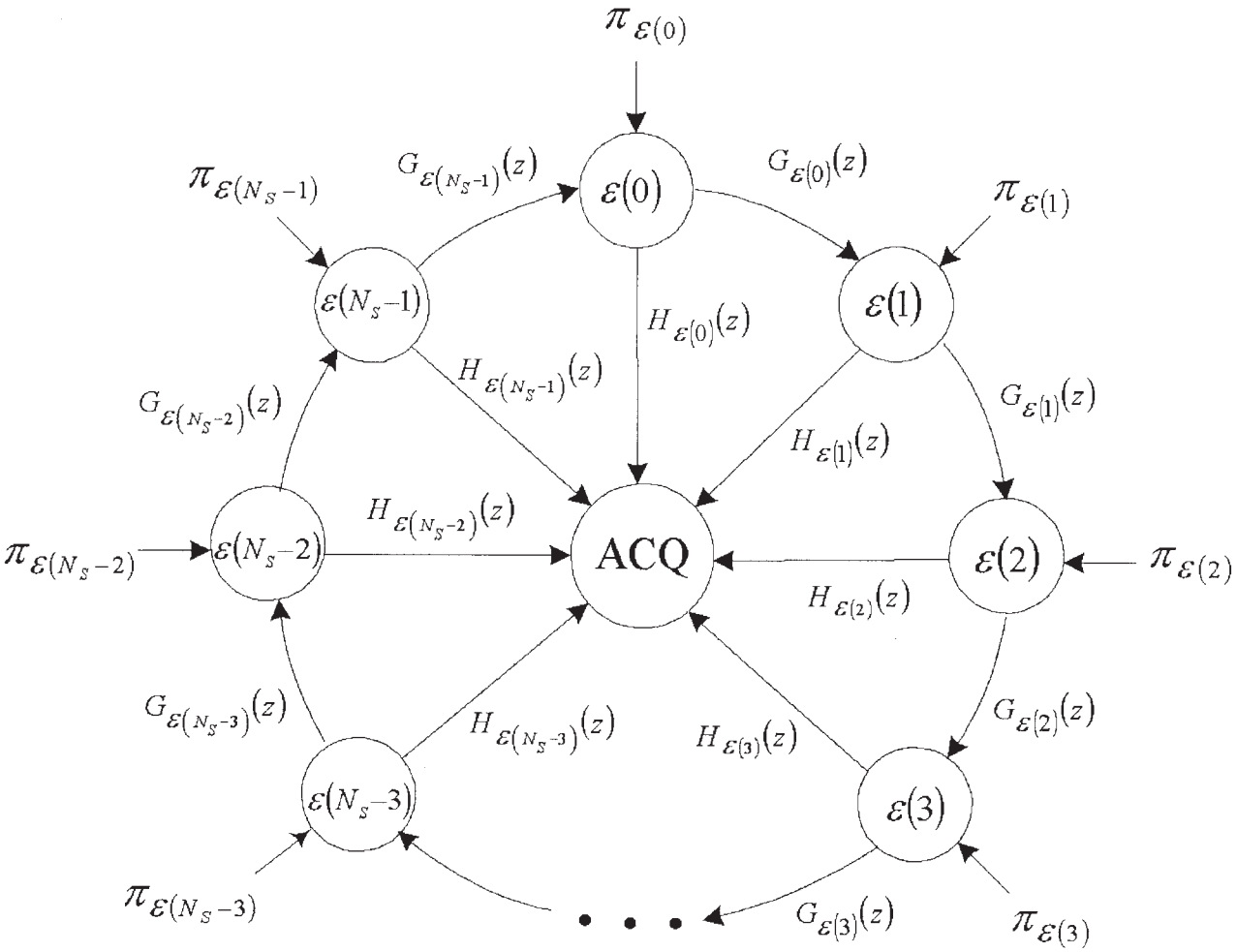

Fig. 1. Generalized acquisition signal flow graph.

graph allows for an arbitrary search permutation $\varepsilon(n)$. An arbitraty detection scenario is also now possible such that any of the states can terminate the search by entering the single trapping state in the middle of the graph, termed the ACQ state. Thus there are $N_s + 1$ states in the flow graph: one trapping state and N_s states representing the bins in the uncertainty region. These bins are labeled $0, 1, \ldots, N_s - 1$, and the specific order in which they are searched is determined by the permutation $\varepsilon(n)$ of the integers $0, 1, \ldots, N_s - 1$. The initial distribution of the states is given by $\pi_{\varepsilon(n)}$. The generating function into the acquisition state can be found by various flow graph loop reduction techniques, Mason's gain formula, and so on, and is given below, where $\oplus$ represents modulo N_s addition and $\prod_{j=0}^{-1}(\cdot)$ is defined to be unity:

$$P_{ACQ}(z) = \frac{\sum_{k=0}^{N_s-1} \pi_{\varepsilon(k)} \sum_{i=0}^{N_s-1} H_{\varepsilon(i\oplus k)}(z) \prod_{j=0}^{i-1} G_{\varepsilon(j\oplus k)}(z)}{1 - \prod_{i=0}^{N_s-1} G_{\varepsilon(i)}(z)}. \quad (1)$$

The path gains $H_{\varepsilon(n)}(z)$ and $G_{\varepsilon(n)}(z)$ are polynomials in the complex variable z and include the transition probabilities and the transition times. For example, a path gain of $0.9z^2$ between any two states means that with probability 0.9 that particular transition occurs and requires 2 "units" of time. The basic unit of time considered here is a single dwell-time, that is, the amount of time an observer dwells on a particular bin when the search is underway. Dwelling longer on a particular bin increases the overall detection probability or decreases the overall false alarm probability depending on whether or not that bin leads to the acquisition state.

The generating function in (1) can be used to determined the probability that the search correctly terminated simply by setting $z = 1$. It also yields a complete statistical description of the acquisition time through the inverse transform relation:

$$p_{ACQ}(n) = \frac{1}{2\pi j} \oint \frac{P_{ACQ}(z)}{z^{n+1}} dz \quad (2)$$

where $p_{ACQ}(n)$ is the probability mass function of the acquisition time (in integer multiples of the dwell-time) and the contour of integration is a counterclockwise closed circular contour in the region of convergence of $P_{ACQ}(z)$ centered around the origin of the complex plane. Typically, only the first few moments of the acquisition time are analyzed for a specific problem and are related to the first few derivatives of the generating function. In this document only the mean search time is examined, which can be computed as:

$$E(T_{ACQ}) = \frac{d}{dz} P_{ACQ}(z)\Big|_{z=1}. \quad (3)$$

A general sequence design problem can now be formulated, even though a solution in the general case seems, at best, very difficult to obtain. Namely, the minimum mean search time can be found from the right choice of search sequence:

$$\varepsilon_{min}(n) = \arg\min_{\varepsilon(n)} E\left(T_{ACQ}|\varepsilon(n)\right). \quad (4)$$

Several specific examples are now considered to demonstrate the applicability of the generalized signal flow graph and its associated generating function in (1). First consider the classical scenario of [1], in which the search pattern is linear or consecutive, that is, $\varepsilon(n) = n$, and there is only one state leading to the acquisition state. This implies that the path gains, $H_n(z)$, are all zero except for $H_{N_s-1}(z) = H_D(z)$. The path gains between states are set equal to:

$$G_{N_s-1}(z) = H_M(z) \text{ and } G_n(z) = H_F(z) \text{ for } n = 0, 1, \ldots, N_s - 2.$$

This leads to the generating function in (4) of [1], part I:

$$P_{ACQ}^{(LINEAR,1)}(z) = \frac{H_D(z)}{1 - H_M(z) H_F^{N_s-1}(z)} \sum_{i=0}^{N_s-1} \pi_i H_F^{N_s-i-1}(z). \quad (5)$$

Here the superscript on $P_{ACQ}(z)$ represents the search type and the number of detection states, that is, (LINEAR,1) means a linear search and one detection state.

A second example is examined in [4] in which L consecutive states $(0, 1, \ldots, L-1)$ lead to the acquisition state and the search pattern is again linear, $\varepsilon(n) = n$. Thus the path gains are $H_n(z) = H_D(z)$ for $n = 0, 1, \ldots, L-1$ and zero for other n while $G_n(z) = H_M(z)$ for $n = 0, 1, \ldots, L-1$ and $G_n(z) = H_F(z)$ for all other n. The prior initial distribution of the states is uniform, $\pi_n = 1/N_s$ for all n. Using (1) with these path gains and initial distribution leads to the generating function in (3) of [4]:

$$P_{ACQ}^{(LINEAR,L)}(z) = \frac{1}{N_s} \cdot \frac{H_D(z)}{1 - H_M^L(z) H_F^{N_s-L}(z)} \Big[\sum_{j=0}^{L-1} H_M^j(z) \sum_{i=0}^{N-L} H_F^i(z) + \sum_{i=1}^{L} \left[L - i + (i-1) H_F^{N_s-L}(z)\right] . H_M^{i-1}(z) \Big]. \quad (6)$$

As one final example, it is noted that the generating function found in [3] also can be found using the generalized

flow graph of Figure 1. The search permutation found in that particular reference, here termed the *look and jump* search, as in [8], is discussed in more detail below.

The mean acquisition time can be found from the generating function of (1) as:

$$E(T_{ACQ}) = \frac{d}{dz} P_{ACQ}(z)\bigg|_{z=1} = \frac{Num' \cdot Den - Num \cdot Den'}{Den^2}. \quad (7)$$

where *Num* and *Den* are the numerator and denominator of (1), respectively, evaluated at $z = 1$. *Num′* is the derivative of the numerator evaluated at $z = 1$:

$$Num' = \sum_{k=0}^{N_s-1} \pi_{\varepsilon(k)} \sum_{i=0}^{N_s-1} \Big(\prod_{j=0}^{i-1} G_{\varepsilon(j\oplus k)}(1)\Big) \cdot \Big[H'_{\varepsilon(i\oplus k)}(1) + H_{\varepsilon(i\oplus k)}(1) \sum_{l=0}^{i-1} \frac{G'_{\varepsilon(l\oplus k)}(1)}{G_{\varepsilon(l\oplus k)}(1)}\Big] \quad (8)$$

Here the summation $\sum_{l=0}^{-1}(\cdot)$ is defined as zero. *Den′* is the derivative of the denominator evaluated at $z = 1$:

$$Den' = -\sum_{i=0}^{N_s-1} \frac{G'_{\varepsilon(i)}(1)}{G_{\varepsilon(i)}(1)} \cdot \prod_{j=0}^{N_s-1} G_{\varepsilon(j)}(1). \quad (9)$$

Figure 2 gives an example of the mean search time, $E(T_{ACQ})$, for three different search patterns, K consecutive detection states, $N_s = 16$, and the path gains, as follows:

$$H_{\varepsilon(i)}(z) = \begin{cases} P_D z & \text{if } i \in I \\ 0 & \text{else} \end{cases}. \quad (10)$$

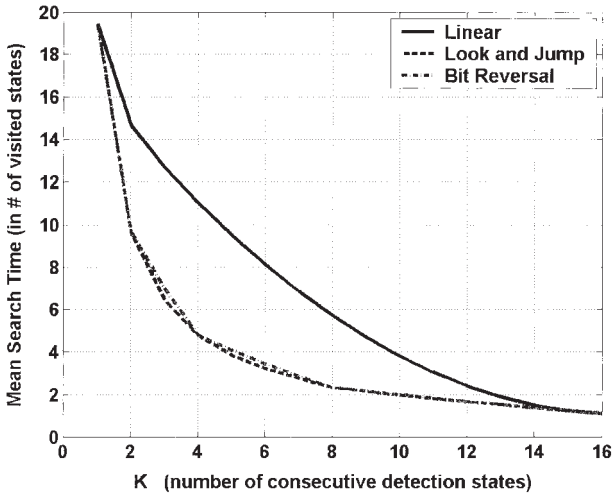

Fig. 2. Mean acquisition time for $P_D = 0.9$, $P_{FA} = 0.1$, $N_s = 16$ and a false alarm penalty time of $J = 10$.

and

$$G_{\varepsilon(i)}(z) = \begin{cases} (1 - P_D)z & \text{if } i \in I \\ (1 - P_{FA})z + P_{FA} z^{J+1} & \text{else} \end{cases}. \quad (11)$$

The index set, I, represents those indices i of $\varepsilon(i)$ that lead to the acquisition state. Here these states are assumed to be $0, 1, \ldots, K-1$ so that the size of the set I is K. Because $\varepsilon(j)$ is simply a permutation of the integers, its inverse $\varepsilon^{-1}(j)$ exists and can be used to produce the index set. That is, $I = \{\varepsilon^{-1}(0), \varepsilon^{-1}(1), \ldots, \varepsilon^{-1}(K-1)\}$ for the example currently being considered, namely K consecutive detection states. The false alarm penalty time is shown in the path gains to be J dwell-times, where J is a known value. This represents a deterministic amount of time, via some level of verification, that is added to the overall search time at every occurrence of a false alarm. In practice the verification phase produces a random penalty time but in order to simplify the acquisition problem it is often assumed to be fixed. Section 8, which deals with fine acquisition, discusses the process of verification in a little more detail.

The search permutations shown in Figure 2 are the *linear, look and jump*, and *bit reversal* searches. The linear search, as mentioned above, is simply a consecutive search with $\varepsilon(n) = n$. The index set for this linear case is $I = \{0, 1, \ldots, K-1\}$. The look and jump search is the permutation $0, K, 2K, \ldots, 1, K+1, 2K+1, \ldots$ with the index set being computed as discussed earlier. For example, when $K = 3$ the index set is seen to be $I = \{0, 6, 11\}$ for $N_s = 16$. As it turns out, the look and jump search is the optimum serial search permutation for K consecutive detection states. However, one issue with this type of search is that K, which must be known to generate this search permutation, is related to the number of detectable paths in the multipath channel for the UWB acquisition problem. As will be discussed in the next section, this quantity may not be known to the receiver.

In lieu of this fact, a class of searches is introduced that yield minimum mean search times but do not require knowledge of K. The searches are known as the *base-b reversal searches*. For example, the $b = 2$, or bit, reversal search is the specific permutation obtained from a bit reversal of the binary representation of the integers $0, 1, \ldots, N_s - 1$, assuming N_s is a power of 2. For $N_s = 16$, the bit reversal search pattern is (in binary) 0000, 1000, 0100, 1100, ..., 0111, 1111 or (in decimal) 0, 8, 4, 12, ..., 7, 15. The index set for the bit reversal search is the first K elements of the bit reversal search permutation, namely $I = \{0, 8, 4, 12, \ldots\}$, because this permutation is its own inverse.

As can be seen in Figure 2, the bit reversal search and the look and jump search yield identical mean acquisition times when K is a power of 2 and the two search schemes

yield very similar acquisition times for all other values of K. In fact, the mean acquisition time is linear in K between values where K is a power of 2. Similarly, it can also be shown that the base b reversed indices yield minimum search times when K and N are powers of b. The $b = 2$ case is well suited for digital architectures and also has an advantage over base-b reversal searches for $b > 2$. Specifically, for a fixed N there are more points in the range $K = 1, \ldots, N$ that are powers of 2 than any other power. Thus when K is not known an appropriate search permutation for minimizing the mean search time is the bit reversal search. As will be seen in Section 5, the bit reversal search also yields an optimum hybrid search when multiple observers are introduced given that K is unknown.

3. UWB SYSTEM OVERVIEW

Before the results of the previous section are applied to study UWB acquisition, the signal and channel models must first be discussed. The pulse shape at the receiver is a 2nd derivative Gaussian pulse:

$$p(t) = \sqrt{\frac{4}{3\sigma\sqrt{\pi}}}\left(1 - \left(\frac{t}{\sigma}\right)^2\right)\exp\left(-\frac{1}{2}\left(\frac{t}{\sigma}\right)^2\right). \quad (12)$$

This pulse has unit energy and the scale factor, σ, which determines the pulse width in time, will be set equal to $\left(2\sqrt{\pi}\right)^{-1} \cdot 0.95$ ns. This propagation model is very simplistic, but will suffice for the present purpose. For detailed propagation studies of UWB signals see [9] or [10] and the references therein.

The multipath channel assumed here is specular and has the impulse response:

$$h(t) = \sum_{l=0}^{L_p-1} \alpha_l \delta(t - \tau_l). \quad (13)$$

The multipath channel considered here is assumed to be static and is based upon a single realization of a UWB channel. This single realization is a measured UWB signal in an office environment as was done in [8]. The amplitude coefficients and time delays, which are ordered so that $\tau_0 < \tau_1 < \ldots$, are thereby also fixed. The worst case multipath channel (channel model 4) in the IEEE 802.15.SG3a channel model final report [11] produces single realizations which are comparable to the one assumed here. At the channel output the received signal, without any data modulation, is:

$$r(t) = \sqrt{E_p}\sum_n \sum_{l=0}^{L_p-1} a_l \cdot p(t - nT_f - c_nT_c - \tau_l) + n(t). \quad (14)$$

The mean zero Guassian random process, $n(t)$, is additive noise with autocorrelation function $N_0\delta(t_1 - t_2)$. The time hopping code assumed here, c_n, is a length N_c sequence of nonnegative integers and T_c is the code chip time. The frame time, T_f, is assumed to be an integer multiple of the code chip time so that $T_f = N_fT_c$. The receiver and transmitter frame times are assumed equal while the transmitter/receiver separation is not known. This gives rise to a uniformly random direct-path arrival-time over the period of the received signal, thus implying that the direct path delay, τ_0, is uniform on $(0, N_cT_f)$.

At the receiver, a group of M correlators is present, with received signal in (14) acting as the input to each of these correlators. It is assumed that there are at least as many arrival paths as there are correlators, that is, $M < L_p$. The received signal is multiplied by an individual correlator template waveform, which for the m-th correlator is:

$$l^{(m)}(t) = \sum_j \sum_{k=0}^{N_c-1} p(t - \alpha_{j,k}^{(m)} - jN_cT_f). \quad (15)$$

The time offset for the m-th correlator template can can vary over a code period and is set by the term $\alpha_{j,k}^{(m)}$. This term is defined as:

$$\alpha_{j,k}^{(m)} = ((kN_f + c_k + k_{\beta,j}^{(m)}) \bmod N_fN_c)T_c + \beta_{r,j}^{(m)}. \quad (16)$$

Proper code phase is accounted for with this term, as well as the proper timing offset within each frame for an arbitrary time shift of $\beta_j^{(m)} = k_{\beta,j}^{(m)}T_c + \beta_{r,j}^{(m)}$, which varies over $[0, N_cT_f)$. The integer term $k_{\beta,j}^{(m)}$ is a nonnegative integer and the remainder term $\beta_{r,j}^{(m)}$ varies over $[0,T_c)$. The frame time is divided into N bins so that $\beta_j^{(m)}$ can be selected from a set of $N \cdot N_c$ time offsets.

As discussed earlier, the codes considered here are short codes so that the correlator dwell-time is one code period in length. Straightforward analysis reveals the output of the m-th correlator: $z_j^{(m)} = s_j^{(m)} + n_j^{(m)}$, where the correlator noise sequence $(n_j^{(m)})$ is an i.i.d. sequence of mean zero, variance N_cN_0 Gaussian random variables. The correlator output mean is:

$$s_j^{(m)} = \sqrt{E_p}\sum_{n=(j-1)N_c}^{(j+1)N_c-1}\sum_{k=0}^{N_c-1}\sum_{l=0}^{L_p-1} a_l \cdot \gamma(\tau_l - \alpha_{j,k}^{(m)} + c_{(n \bmod N_c)}T_c - (jN_c - n)T_f), \quad (17)$$

where the pulse autocorrelation function of (12) is:

$$\gamma(\tau) = \left(1 - \left(\frac{\tau}{\sigma}\right)^2 + \frac{1}{12}\cdot\left(\frac{\tau}{\sigma}\right)^4\right)\exp\left(-\frac{1}{4}\cdot\left(\frac{\tau}{\sigma}\right)^2\right). \quad (18)$$

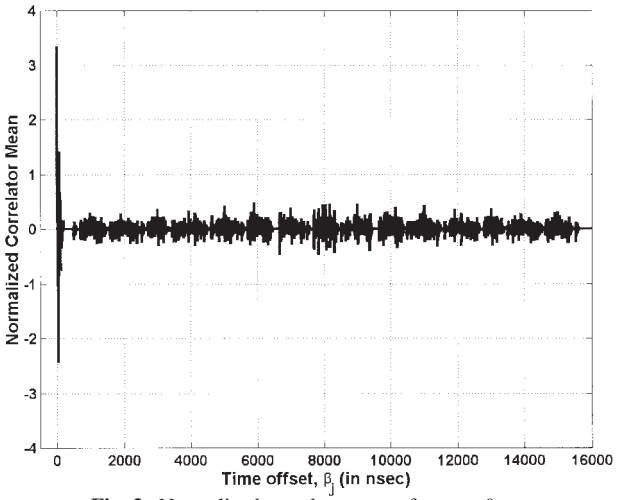

Fig. 3. Normalized correlator mean for $\tau_0 = 0$ ns.

Now an example of the correlation mean, normalized by $\sqrt{E_p}$, is shown, where it is assumed that $T_c = 10$ ns, $T_f = 1000$ ns, $N_f = 100$, $N_c = 16$, and $N = 256$. The normalized correlation mean, computed at each of the bin centers for $\beta_j = j \cdot T_f/N$ with $j = 0, 1, \ldots, N \cdot N_c - 1$, is shown in Figure 3 for $\tau_0 = 0$ ns. The code sequence, $\{c_n\}_{n=0}^{N_c-1} = \{0, 13, 52, 43, 61, 30, 26, 48, 21, 21, 48, 26, 30, 61, 43, 52\}$. This code sequence is based upon techniques found in [12] and is a sequence of integers between 0 and 70, where the maximum value of 70 provides some guard time in each frame. A method of code design for rapid acquisition is studied in [13] for a slightly different modulation scheme.

4. UWB ACQUISITION ANALYSIS

The generalized signal flow graph approach is now used to study the acquisition of an UWB signal in dense multipath. The code length and the number of bins per frame are set as in the previous section; thus there are $N_s = N \cdot N_c = 256 \cdot 16 = 4096$ bins in the uncertainty region. The code chip time and the frame time are $T_c = 10$ ns and $T_f = 1000$ ns, respectively, as in the last section and the code sequence and multipath channel are also unchanged. Thus the normalized correlator mean of (17) and shown in Figure 3 is now used. The acquisition process considered here uses a single correlator and detection occurs when the correlator output crosses a predetermined threshold. This is extended in the next section to use multiple correlators for the hybrid search.

The correlator output, $z_j = s_j + n_j$, is Gaussian with mean s_j and variance $N_c N_0$. The probably of exceeding the threshold for the j-th code correlator output for a detection threshold of $\Upsilon \cdot \sqrt{E_p}$ where Υ is the normalized detection threshold, is:

$$\begin{aligned} P_{\varepsilon(j)} &= \Pr(|z_j| > \Upsilon \cdot \sqrt{E_p}) \\ &= Q\left(\sqrt{\frac{E_p}{N_c N_0}} \cdot (\Upsilon + \frac{s_j}{\sqrt{E_p}})\right) \\ &\quad + Q\left(\sqrt{\frac{E_p}{N_c N_0}} \cdot (\Upsilon - \frac{s_j}{\sqrt{E_p}})\right). \end{aligned} \tag{19}$$

The quantity s_j is given in (17), and the function $Q(x)$ is the Gaussian integral function. The permutation $\varepsilon(j)$ of the integers $0, 1, \ldots, N \cdot N_c - 1$ is related to the search variable β_j as:

$$\beta_j = \varepsilon(j) \cdot T_f/N\,. \tag{20}$$

The initial distribution is set by the uniform nature of the direct path arrival time, τ_0, so that $\pi_{\varepsilon(j)} = 1/(N \cdot N_c)$. In the next section an alternative method of setting the initial distribution is examined. The signal flow graph path gains in Figure 1 are

$$H_{\varepsilon(j)}(z) = \begin{cases} P_{\varepsilon(j)} z & \text{if } j \in I \\ 0 & \text{else} \end{cases} \tag{21}$$

and

$$G_{\varepsilon(j)}(z) = \begin{cases} (1 - P_{\varepsilon(j)})z & \text{if } j \in I \\ (1 - P_{\varepsilon(j)})z + P_{\varepsilon(j)} z^{J+1} & \text{else} \end{cases}. \tag{22}$$

The index set I is selected based on the number of detectable paths in the multipath channel and for simplicity was selected as the first $K = 50$ bins. This assumption of K consecutive bins is a reasonable assumption since the arrivals are clustered, even though some paths within the cluster are small in amplitude. The mean search time in (8) is shown in Figure 4. Here the normalized detection threshold (Υ) is optimized for minimum mean acquisition time at each E_p/N_0. Again, J is the false alarm penalty time.

5. HYBRID SERIAL/PARALLEL SEARCH ANALYSIS

A fully parallel search would minimize the mean acquisition time but is often too complex to actually implement. Even for the short code length ($N_c = 16$) in the last section, $N \cdot N_c = 4096$ correlators are required to implement a parallel search. A hybrid search offers a reasonable trade-off between acquisition time and receiver complexity. It is intuitively obvious that multiple correlators will always reduce the mean acquisition time ver-

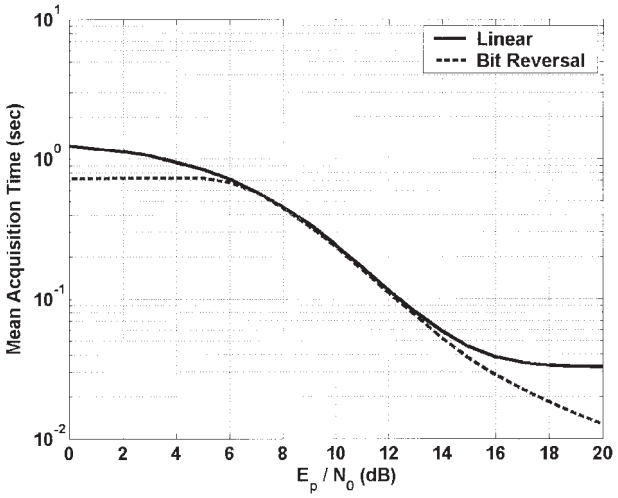

Fig. 4. Mean UWB acquisition time for a single correlator, T_f = 1000 nsec, T_c = 10 ns, N = 256, N_c = 16, J = 1000, and optimized threshold, Y.

sus a single correlator because each correlator can search a different code phase. It also seems reasonable that the individual correlator search patterns should not be independent of one another. In fact, dividing a single search permutation amongst multiple correlators provides an optimum method of searching the entire uncertainty region as quickly as possible with no redundancy.

The bit reversal search pattern, being the optimum search permutation without knowledge of K, is now divided amongst M correlators. The permutation can be listed as $\beta_0, \beta_1, \beta_2, \ldots, \beta_{N \cdot N_c - 1}$. Then the first correlator is assigned to search as per $\beta_j^{(0)} = \{\beta_0, \beta_M, \beta_{2M}, \ldots\}$, the second correlator searches as per $\beta_j^{(1)} = \{\beta_1, \beta_{M+1}, \beta_{2M+1}, \ldots\}$, and so on. If M and $N \cdot N_c$ are both powers of 2, then M divides $N \cdot N_c$ into smaller regions of N_h bins, where N_h is also power of 2. Each correlator then performs a bit reversal search over this smaller region of N_h bins. Figure 5 shows an example of this phenomenon for N_s = 16 search bins and M = 4 correlators. This same phenomenon is also exhibited for other base b reversal searches when both N_s and M are powers of b.

The generating function for the hybrid search can be computed from the generalized acquisition signal flow graph in Figure 1. Before this generating function is found, an alternative method of determining the mean acquisition time is given. Specifically, the initial distribution of the signal flow graph is set to $\pi_{\varepsilon(0)} = 1$ and $\pi_{\varepsilon(j)} = 0$ for all $j \neq 0$ so that the search always starts in state $\varepsilon(0)$. The resulting generating function is conditional on the set of states, $\boldsymbol{K} = [k_1, k_2, \ldots, k_K]^T$, that lead into the acquisition state:

$$P_{ACQ}(z|\boldsymbol{K}) = \frac{\sum_{i=0}^{N_s-1} H_{\varepsilon(i)}(z) \prod_{j=0}^{i-1} G_{\varepsilon(j)}(z)}{1 - \prod_{i=0}^{N_s-1} G_{\varepsilon(i)}(z)}. \qquad (23)$$

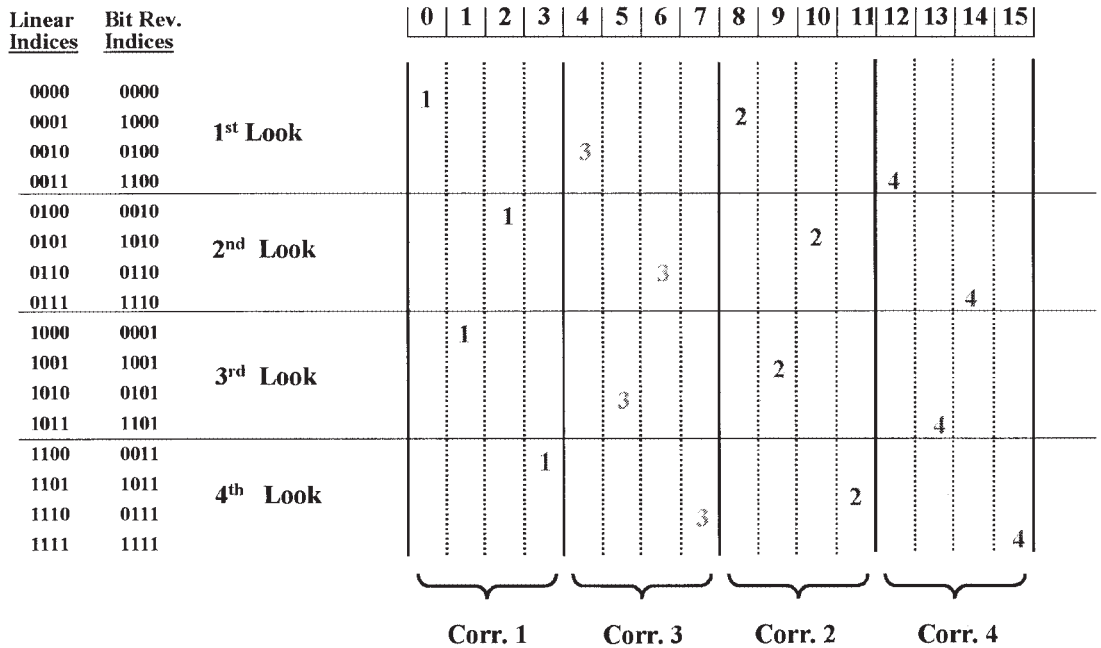

Fig. 5. Hybrid bit reversal search example for N_s = 16 bins and M = 4 correlators.

The dependence of this conditional generating function on the set $\boldsymbol{K}$ occurs via the path gains, $H_{\varepsilon(j)}(z)$ and $G_{\varepsilon(j)}(z)$, which are both inherently functions of $\boldsymbol{K}$. The mean search time found from the conditional generating function is also conditional on the set $\boldsymbol{K}$, and the overall mean search time is found as $E(T_{ACQ}) = E(E(T_{ACQ} \mid \boldsymbol{K}))$, where the outer expectation is with respect to $\boldsymbol{K}$. If the first component of $\boldsymbol{K}$ is uniform on the integers from 0 to $N_s - 1$ while the other values are simply some known offset away from the first random component then the mean search time can be computed as:

$$E(T_{ACQ}) = \frac{1}{N_s} \sum_{k_1=0}^{N_s-1} E(T_{ACQ}|k_1)\,. \tag{24}$$

The conditional mean, $E(T_{ACQ} \mid k_1)$, is computed as the first derivative of the conditional generating function in (23) evaluated at $z = 1$. For the case of the UWB acquisition problem the uniform nature of the direct path arrival time, τ_0, must be incorporated into the mean acquisition time. It is fairly straightforward to show:

$$E(T_{ACQ}) = \frac{1}{N_c \cdot T_f} \int_0^{N_c \cdot T_f} E(T_{ACQ}|\tau_0)\, d\tau_0\,. \tag{25}$$

The first M search locations are $\varepsilon(0)$, $\varepsilon(1)$, . . . , $\varepsilon(M-1)$, the next M locations are $\varepsilon(M)$, $\varepsilon(M+1)$, . . . , $\varepsilon(2M-1)$, etc. It will be assumed that M divides N_s evenly into N_s/M regions. Only after the signal flow graph has exited one of these regions has one dwell-time elapsed, because M correlation outputs are available every dwell-time. This can be expressed by defining a boundary set $B = \{M-1, 2M-1, \ldots, N_s-1\}$ and redefining (22) as:

$$G_{\varepsilon(j)}(z) = \begin{cases} 1 - P_{\varepsilon(j)} & \text{if } j \in I \text{ and } j \notin B \\ (1 - P_{\varepsilon(j)})z & \text{if } j \in I \text{ and } j \in B \\ 1 - P_{\varepsilon(j)} + P_{\varepsilon(j)}z^J & \text{if } j \notin I \text{ and } j \notin B \\ (1 - P_{\varepsilon(j)})z + P_{\varepsilon(j)}z^{J+1} & \text{if } j \notin I \text{ and } j \in B. \end{cases} \tag{26}$$

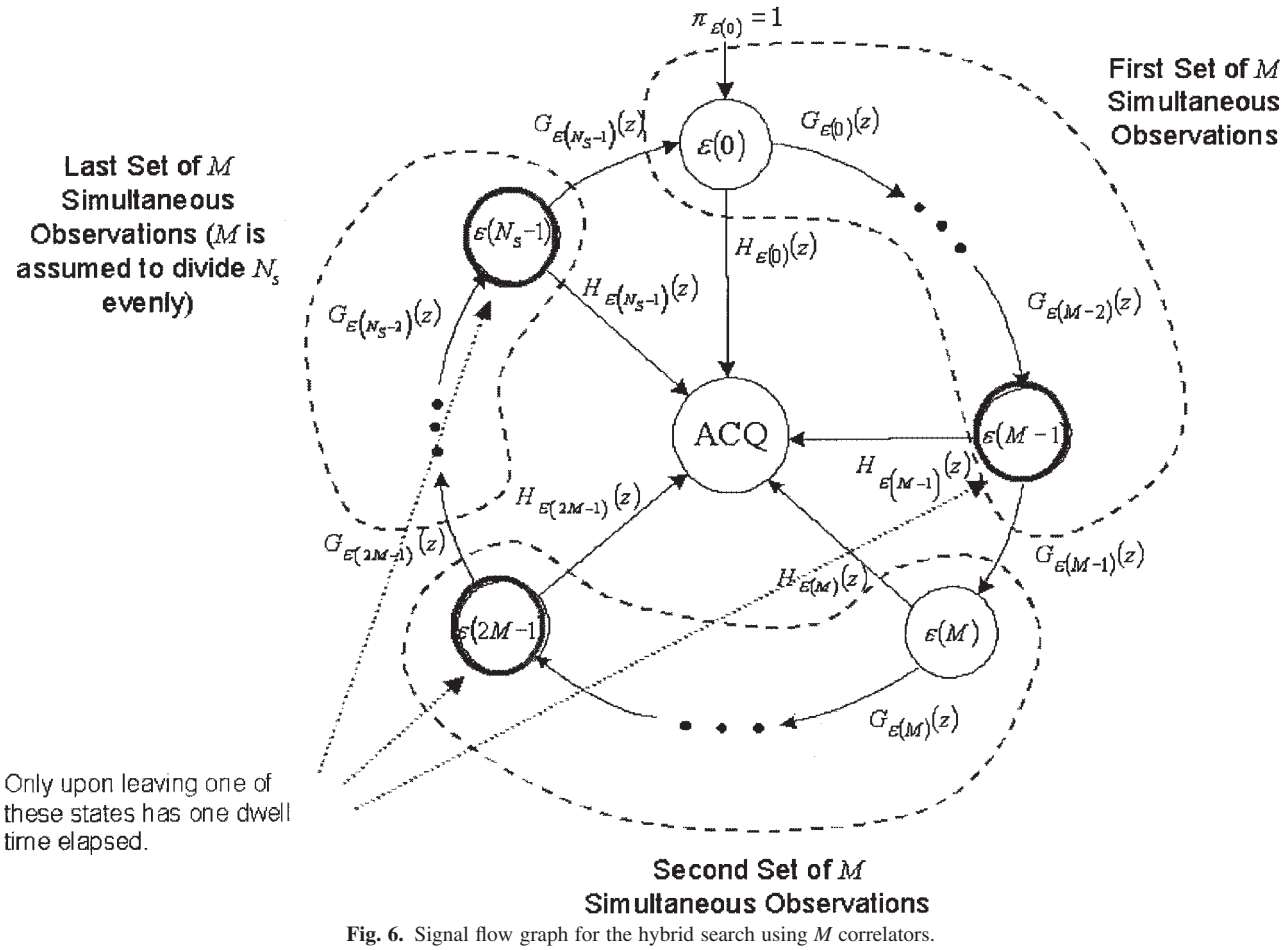

Fig. 6. Signal flow graph for the hybrid search using M correlators.

The path gain $H_{\varepsilon(j)}(z)$ can only be non-zero when $j \in I$ as in (21). The signal flow graph for the hybrid search is seen in Figure 6. Some results for a bit reversal hybrid search example are shown in Figure 7a.

One method of decreasing the acquisition time for the hybrid case is to first sort the M correlator outputs based upon magnitude. The bins are then searched in the order of decreasing magnitude. This idea was first introduced in [14]. The next section discusses this sorted hybrid search.

6. SORTED HYBRID SEARCH

Once the M correlator outputs have been determined, the bin in the uncertainty region corresponding to the largest magnitude is searched first, followed by the second largest magnitude, etc. The acquisition time cannot be computed using the particular signal flow graph discussed earlier because the specific search order now depends upon the outcome of the correlators, which are all random variables. It is possible that a more general framework, obtained by combining Markov Decision Theory and signal flow graphs, could be used to study this type of search. Computer simulations have revealed, as expected, that sorting in this fashion does indeed reduce the acquisition time.

A bound on the sorted hybrid search can be found using the generalized signal flow graph approach of Section 2. This bound is obtained by first searching those cells with the largest transition probabilities into the acquisition state. Specifically this is done by defining a new search order $\varepsilon_s(j)$ where:

$$\begin{aligned}
\varepsilon_s(0) &= \{\varepsilon(j_0) : P_{\varepsilon(j_0)} = \max_{i=0,\ldots,M-1} P_{\varepsilon(i)}\} \\
\varepsilon_s(1) &= \{\varepsilon(j_1) : P_{\varepsilon(j_1)} = \max_{\substack{i=0,\ldots,M-1 \\ i\neq j_0}} P_{\varepsilon(i)}\} \\
&\vdots \\
\varepsilon_s(M-1) &= \{\varepsilon(j_{M-1}) : P_{\varepsilon(j_{M-1})} = \min_{i=0,\ldots,M-1} P_{\varepsilon(i)}\} \\
\varepsilon_s(M) &= \{\varepsilon(j_M) : P_{\varepsilon(j_M)} = \max_{i=M,\ldots,2M-1} P_{\varepsilon(i)}\} \\
\varepsilon_s(M+1) &= \{\varepsilon(j_{M+1}) : P_{\varepsilon(j_{M+1})} = \max_{\substack{i=M,\ldots,2M-1 \\ i\neq j_M}} P_{\varepsilon(i)}\} \\
&\vdots \\
\varepsilon_s(2M-1) &= \{\varepsilon(j_{2M-1}) : P_{\varepsilon(j_{2M-1})} = \min_{i=M,\ldots,2M-1} P_{\varepsilon(i)}\} \\
&\vdots
\end{aligned} \tag{27}$$

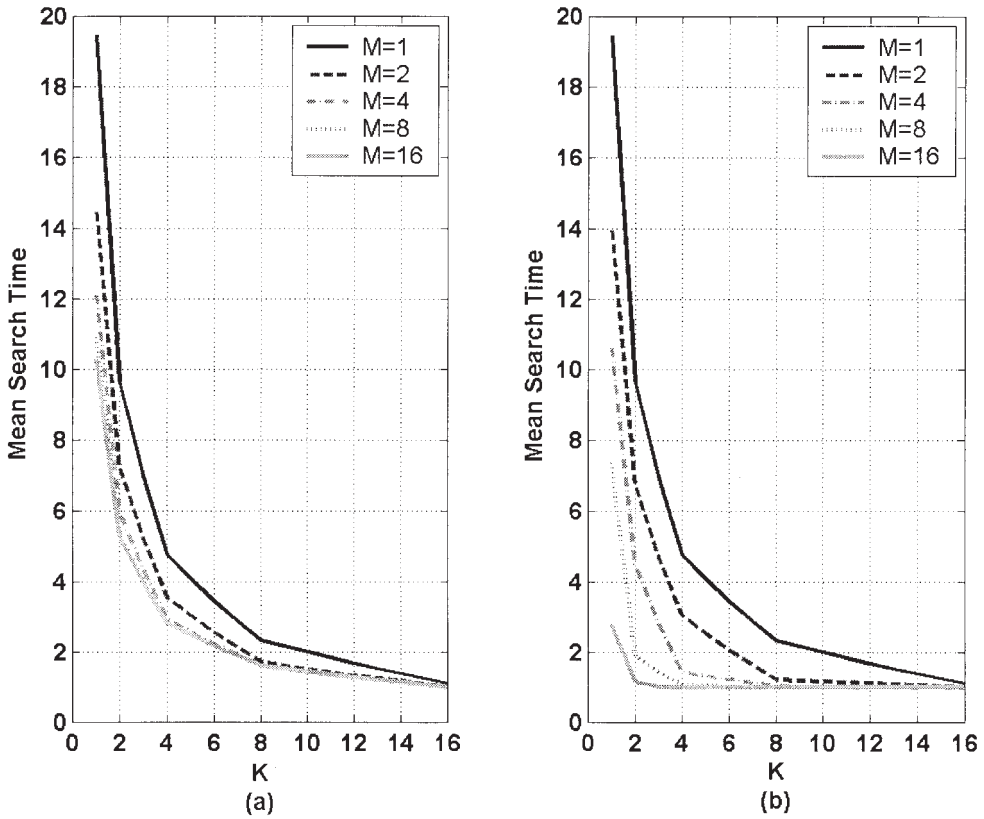

Fig. 7. Bit reversal search mean acquisition time for the (a) hybrid case of M correlators and (b) the corresponding sorted hybrid bound for K consecutive detection bins, $P_D = 0.9$ and $P_{FA} = 0.1$ for each bin, $N_s = 16$, and a false alarm penalty time of $J = 10$.

The signal flow graph and thus the generating function from the previous section are now updated with $\varepsilon_s(j)$ replacing $\varepsilon(j)$. Figure 7 shows some hybrid bit reversal search results for a very simple case of $N_s = 16$ bins each, with a certain detection and false alarm probability, P_D and P_{FA}, as was done in Section 2. The associated bound on the sorted hybrid search is also shown.

7. BOUND ON MEAN SEARCH TIME FOR A SINGLE OBSERVER

This section briefly discusses the possibility of a single observer nearly attaining the search performance of two observers. Recall that an observer is the object performing the search, for example, the correlator in the last section. A single observer bound under perfect conditions ($P_D = 1$ and $P_{FA} = 0$) is derived based upon Markov's inequality and compared to an $M = 2$ hybrid bit reversal search for the same perfect conditions. It is seen that the single observer bound sits just above the two observer hybrid bit reversal search mean acquisition time.

Markov's inequality for a random variable, X, states that if $X \geq 0$ and $\alpha > 0$, then:

$$\Pr(X \geq \alpha) \leq \frac{E(X)}{\alpha} \tag{28}$$

If the random variable is assumed to be the search time, $X = T_{ACQ}$, and $\alpha = 1, 2, \ldots, N_s - K + 1$, with the probability $\Pr(T_{ACQ} \geq \alpha)$ computed directly then repeated application of Markov's inequality yields the greatest lower bound on the mean search time:

$$E(T_{ACQ}) \geq \max_{1 \leq k \leq N_s - K + 1} \left(k \cdot \prod_{j=0}^{k-2} \left(1 - \frac{1}{N_s - j} \right) \right) \tag{29}$$

As before $\Pi_{j=0}^{-1}(\cdot)$ is defined to be unity, N_s is the number of search locations, or bins, and K is the number of consecutive locations that will terminate the search. The single observer bound is shown in Figure 8 along with the hybrid bit reversal search results for the case of $N_s = 16$. It is seen that indeed the bound on single observer performance is very near but slightly above the two observer case. In fact, this same phenomenon was observed for a wide range of scenarios involving different values of N_s. This raises the question: Does a single observer search pattern exist such that the mean search time approaches that of two observers?

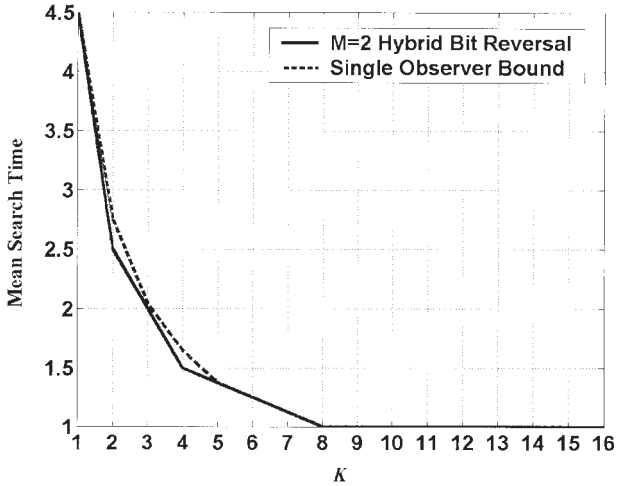

Fig. 8. Comparison of the mean search time for the single observer bound versus the two observer hybrid bit reversal search ($P_D = 1$, $P_{FA} = 0$).

8. FINE ACQUISITION AND THE SELF-SIMILAR SIGNAL FLOW GRAPH

The acquisition process described up to this point has only determined the location of the *group* of bins in the uncertainty region, e.g., for the UWB acquisition problem the multipath "cluster" has been located. This can be termed *coarse acquisition*. The process of *fine acquisition* is now briefly discussed, which is simply finalizing the locations of the M strongest paths within the multipath cluster of arrival paths.

At the start of the fine acquisition process it is known that a single path within the cluster of paths has been located. Measurements of UWB channels has revealed that different paths arrive in the same general temporal neighborhood at the receiver, that is, they tend to cluster in groups. Thus the M strongest paths that have arrived at the receiver should be in the vicinity of the coarse acquisition termination point. Some level of *verification* is always required to ensure that acquisition has indeed occurred. Up to this point a perfect verification phase has been assumed, which introduces a fixed delay of J dwell times to the overall code acquisition time when a false alarm is encountered. The simplest verification phase would involve dwelling for an extended length of time so as to increase the probability of correct acquisition. This concept is now extended for the case of multiple correlators that are perturbed around the coarse acquisition termination point.

Figure 9 shows an example of the fine acquisition process. The coarse acquisition point has terminated at the bin, n_c, which corresponds to a time offset of $n_c \cdot \frac{T_f}{N}$.

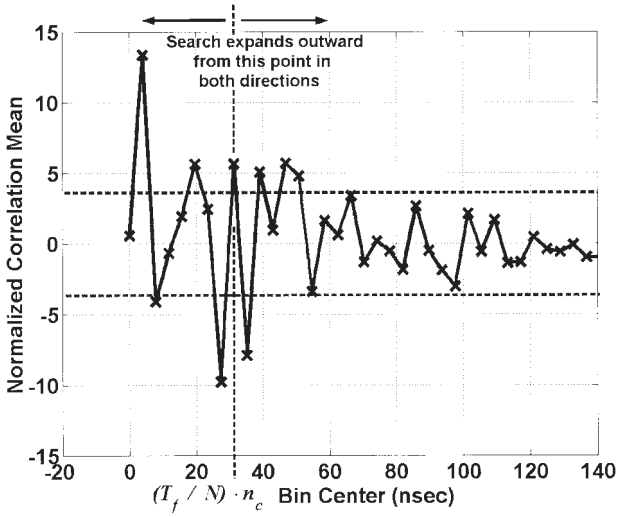

Fig. 9. Normalized correlator mean for a code length of $N_c = 64$. The coarse acquisition termination point is denoted as n_c, which is the starting point for fine acquisition.

The M correlators then search the neighboring bins, going outward away from n_c until some stopping criterion is satisfied. Generally, an upper bound, say $\pm J_1$, is set on the distance that can be traveled before declaring a false alarm and returning to coarse acquisition. This upper bound directly affects the false alarm penalty time, as does the specific stopping criterion used.

The m-th correlator output is defined as $z_j^{(m)} = s_j^{(m)} + n_j^{(m)}$ for $m = 0, 1, \ldots, M-1$. The correlator mean is given in (17). Some example stopping criteria include the following:

1. Search in both directions and stop after some fixed offset, for example, $\pm J_2$ where $J_2 < J_1$.
2. Search in both directions until $|z_j^{(m)}| < T$ for all m and for some T.
3. Search in both directions until $\Sigma_m |z_j^{(m)}| < T$ for some T.

Independent of the stopping criterion is a verification criterion, which basically determines if a false alarm has occurred. It is assumed that the largest correlator magnitudes are stored during the fine acquisition process in a vector $\boldsymbol{\nu} = [\nu_0, \nu_1, \ldots, \nu_{M-1}]$, where ν_0 is the largest correlator magnitude seen during the search thus far, ν_1 is the second largest, and so on. Some example verification criteria include the following:

1. Detection has occurred if $\nu_m > T$ for all m and for some T.
2. Detection has occurred if $\Sigma_m \nu_m^n > T$ for some T and $n = 1$ or 2.
3. False alarm has occurred if $\nu_m < T$ for some m and some T.

No matter which stopping or verification criteria are employed, the problem is still basically the same. Namely, a hybrid search with $N_s = 2J_1$ states is conducted so that the generalized signal flow graph approach can again be used. In this case, the path gains are now functions of the specific stopping and verification criteria.

As an example consider stopping criterion (1) with a verification criterion of (1). Assuming that M divides $2J_2$ evenly, the hybrid signal flow graph of Figure 6 can be used, where $G_{\varepsilon(n)}(z) = 1$ for all $n \notin B$ and $G_{\varepsilon(n)}(z) = z$ for all $n \in B$ where $B = \{M, 2M, \ldots\}$. Finally the path gains for the state $\varepsilon(2J_2 - 1)$ are given as:

$$H_{\varepsilon(2J_2-1)}(z) = z \cdot \Pr\left(\bigcap_{m=0}^{M-1} \nu_m > T\right)$$

$$G_{\varepsilon(2J_2-1)}(z) = z \cdot \left(1 - \Pr\left(\bigcap_{m=0}^{M-1} \nu_m > T\right)\right). \quad (30)$$

The overall process of UWB acquisition includes coarse and fine acquisition. The overall signal flow graph representing this search process is seen in Figure 10 and is termed a self-similar signal flow graph, for obvious reasons. Once coarse acquisition has terminated, fine acquisition begins where coarse acquisition left off, giving rise to the self-similar nature of the graph. If the fine acquisition process is collapsed into two individual path gains, one leading to the ACQ state and one leading to the next coarse acquisition state, the the resulting graph is simply the generalized signal flow graph of Figure 1.

9. CONCLUSIONS

A generalized signal flow graph and the associated moment generating function, suitable for studying a large class of search problems, were presented in this paper. This flow graph approach was used to study acquisition of a UWB signal in a dense multipath channel. Hybrid serial/parallel search schemes were investigated, as well as sorted hybrid search schemes. The hybrid bit reversal search was shown to be optimum under certain conditions. Finally, fine acquisition was investigated using the signal flow graph approach for arbitrary stopping and verification criteria. The concatenation of coarse acquisition and fine acquisition into a single graph led to the concept of a self-similar signal flow graph.

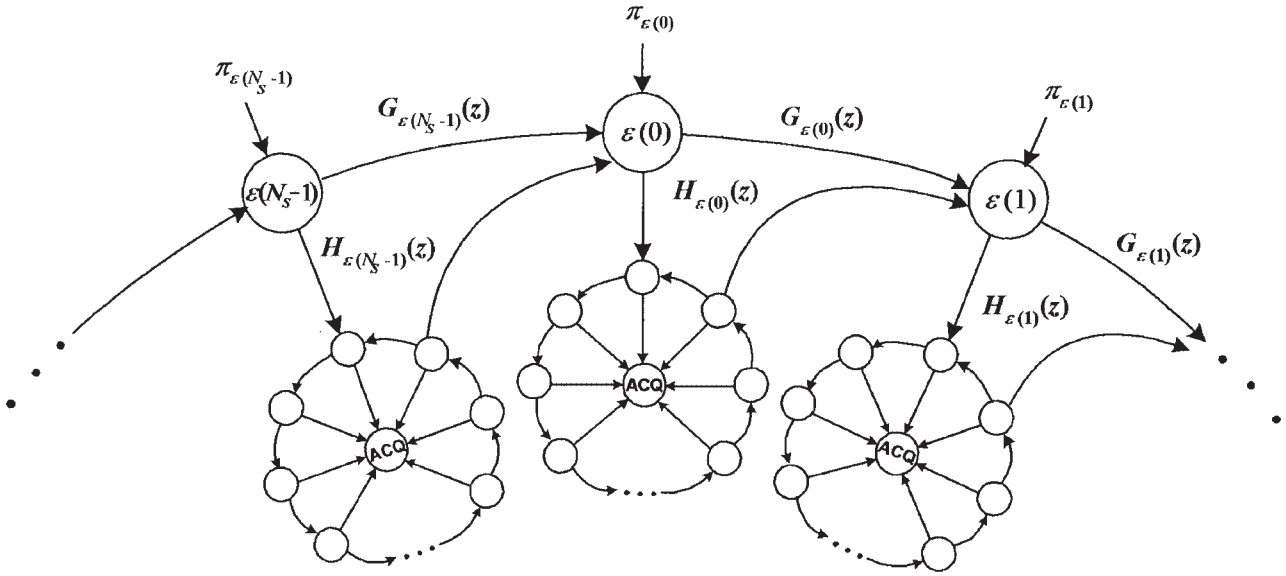

Fig. 10. Self-similar signal flow graph.

ACKNOWLEDGMENTS

This work was supported in part by the Department of Defense under MURI Grant No. DAAD19-01-1-0477 and in part by a NGST Doctoral Fellowship.

REFERENCES

1. A. Polydoras and C. Weber, A unified approach to serial search spread-spectrum code acquisition. I and II, *IEEE Transactions on Communication*, Vol. 32, No. 5, pp. 542–560, 1984.
2. E. A. Homier and R. A. Scholtz, Hybrid fixed-dwell-time search techniques for rapid acquisition of ultra-wideband signals, *Proceedings of the International Workshop on Ultra-Wideband Systems*, June 2003.
3. O.-S. Shin and K. Bok Lee, Utilization of multipaths for spread-spectrum code acquisition in frequency-selective Rayleigh fading channels, *IEEE Transactions on Communication*, Vol. 49, pp. 734–743, 2001.
4. J. Iinatti, Mean acquisition time of DS code acquisition in fixed multipath channel, *IEEE 5th International Symposium on Spread Spectrum Techniques and Applications*, Vol. 1, pp. 116–120, 1998.
5. H.-C. Wang and W.-H. Sheen, Variable dwell-time code acquisition for direct sequence spread spectrum systems on multipath fading channels, *Proceedings of the International Conference on Communications*, Vol. 3, pp. 1232–1236, 1998.
6. H. Zhang, S. Wei, D. Goeckel, and M. Win, Rapid acquisition of ultra-wideband radio signals, *Proceedings of the Asilomar Conference on Signals, Systems, and Computers*, November 2002.
7. M. Zhu and K. Chugg, Iterative message passing algorithms for rapid code acquisition, *Proceedings of the IEEE Military Communication Conference*, October 2003.
8. E. A. Homier and R. A. Scholtz, Rapid acquisition of ultra-wideband signals in the dense multipath channel, *IEEE UWBST2002*, pp. 105–109, May 2002.
9. J. M. Cramer, R. A. Scholtz, and M. Z. Win, Evaluation of an ultra-wideband propagation channel, *IEEE Transactions on Antennas and Propagation*, May 2002.
10. A. Alvarez, G. Valera, M. Lobeira, R. Torres, and J. Garcia, Ultra-wideband channel characterization and modeling, *Proceedings of the International Workshop on Ultra-Wideband Systems*, June 2003.
11. J. Foerster, Channel modeling sub-committee report final, *IEEE 802.15.SG3a Study Group*, December 2002.
12. R. A. Scholtz, P. V. Kumar, and C. J. Corrada-Bravo, Signal design for ultra-wideband radio, *Sequences and Their Applications (SETA'01)*, May 2001.
13. R. Fleming, C. Kushner, G. Roberts, and U. Nandiwada, Rapid acquisition for ultra-wideband localizers, *Proceedings of the IEEE Conference on UWB Systems and Technologies 2002*, May 2002.
14. E. C. Posner, Optimal search procedures, *IRE Transactions on Information Theory*, Vol. 11, pp. 157–160, July 1963.

Eric A. Homier received the B.S. degree in Computer and Electrical Engineering from Purdue University in 1996, where he was a co-op student with Thomson Consumer Electronics and worked on a variety of projects involving, among other things, direct broadcast satellite receiver design and analysis, television tuner design, and indoor wireless remote control design and fabrication. In 1998, he received the M.S. degree in Electrical Engineering from the University of Southern California on a TRW (now Northrop Grumman) Master's Fellowship. In 1999, Mr. Homier became a Northrop Grumman

Doctoral Fellowship student at USC, where he is earning his Ph.D. under the advisement of Dr. Robert Scholtz. Since 1999, Mr. Homier has been working in the Ultra-Wideband Radio Laboratory and has assisted in a variety of channel measurements and interference tests. This work includes ultra-wideband measurements for the Office of Naval Research taken aboard cargo ships, as well as work done for the Department of Defense under a Multi-University Research Initiative. His doctoral research is in the area of synchronization of ultra-wideband signals. Mr. Homier's work at Northrop Grumman Space Technology (formerly TRW) in Redondo Beach, California has been primarily in the area of satellite system engineering and advanced studies on a variety of programs for the U.S. government. Mr. Homier and Dr. Scholtz were recipients of a Best Paper Award at the 2003 International Workshop on Ultra-Wideband Systems.

Robert A. Scholtz is a Distinguished Alumnus of the University of Cincinnati, where, as a Sheffield Scholar, he received the Degree in Electrical Engineer in 1958. He was a Hughes Masters and Doctoral Fellow while obtaining his M.S. and Ph.D. degrees in Electrical Engineering from the University of Southern California in 1960 and Stanford University in 1964, respectively. Dr. Scholtz, working on missile radar signal processing problems, remained part-time at Hughes Aircraft Co. until 1978. In 1963, he joined the faculty of the University of Southern California, where he is now the Fred H. Cole Professor of Engineering. From 1984 through 1989, he served as Director of USC's Communication Sciences Institute, and from 1994 to 2000 he was Chairman of the Electrical Engineering Systems Department. In 1996, as part of the Integrated Media Systems Center effort, Dr. Scholtz formed the Ultrawideband Radio Laboratory (UltRa Lab) to provide facilities for the design and test of impulse radio systems and other novel high-bandwidth high-data-rate wireless mobile communication links. His research interests include communication theory, synchronization, signal design, coding, adaptive processing, and pseudonoise generation, and their application to communications and radar systems. He has co-authored *Spread Spectrum Communications*, the *Spread Spectrum Communications Handbook*, and *Basic Concepts in Information Theory and Coding*. Dr. Scholtz is a Fellow of the IEEE. His paper co-awards include the Leonard G. Abraham Prize from the IEEE Communications Society, the Donald G. Fink Prize Award of the IEEE, the 1992 Senior Award of the IEEE Signal Processing Society, the Ellersick Award from Milcom'97, the Schelkunoff Prize from the IEEE Antennas and Propagation Society, and the Best Paper Award at the 2003 International Workshop on Ultra-Wideband Systems.